

Predicting uniaxial compressive strength of different rocks using principal component analysis and deep neural network

Mojtaba Amiri¹, Mehrdad Amiri², Seyed Sajjad Karrari³, Siamak Moradi⁴

Received: 2024 Nov. 19, Revised: 2025 Feb. 02, Online Published: 2024 Feb. 08



Journal of Geomine © 2024 by University of Birjand is licensed under [CC BY 4.0](https://creativecommons.org/licenses/by/4.0/)

ABSTRACT

Uniaxial compressive strength (UCS) is one of the most practical parameters of rock mechanics. It is an important and basic geomechanical factor in the design of tunnels, dams, and underground drilling. The direct method for determining the UCS in the laboratory is expensive and time-consuming. Therefore, several empirical equations have been developed to estimate the UCS from the results of index and physical tests of rock. Nevertheless, numerous empirical models available in the literature often make it difficult for mining engineers to decide which empirical equation provides the most reliable estimate of UCS. This work aims to estimate the UCS of rocks using a machine learning-based approach. More specifically, a deep neural networks (DNN) model is designed to predict the UCS from the physical and mechanical characteristics of rocks. 221 different rock block samples were collected from various areas of Iran. The physical and mechanical properties include Dry density (ρ), P-wave velocity (V_p), Point load test (I_{S50}), Brazilian tensile strength (BTS), and water absorption (I_w). In order to reduce the dimension of the input features, before the DNN model, principal component analysis (PCA) is employed. A combination of the PCA and the proposed DNN model is found to be efficient and useful in predicting UCS. The mean square error of the proposed method with and without the feature reduction stage was 0.0068 ± 0.001 and 0.0067 ± 0.013 , respectively.

KEYWORDS

Physical and mechanical properties, Uniaxial compressive strength (UCS), Deep neural network (DNN)

I. INTRODUCTION

Uniaxial compressive strength (UCS) is a critical parameter of rocks and is useful for engineering applications such as tunnel and dam design, rock blasting, and underground drilling. This parameter is determined directly based on the standards of the ISRM and ASTM by testing on the intact rock sample. The direct method for determining the UCS in the laboratory is expensive and time-consuming. In addition, the determination of this parameter with high accuracy requires a suitable and high-quality core sample, while it is difficult to obtain an appropriate core from weak and crushed rocks (Fener et al., 2005). In order to avoid these problems, index tests are used to determine the UCS, indirectly. Many researchers have predicted the UCS of different types of rocks using experimental relationships developed by the simple and multiple regression analysis (e.g., Singh and Dubey, 2000; Tiryaki, 2008; Diamantis et al., 2009; Heidari et al., 2012; Kumar et al., 2013; Nefeslioglu, 2013; Ozcelik et al., 2013); Asteris et al., 2024). The predicted UCS parameter is obtained based

on three non-destructive tests. These tests include Schmidt hardness, density, and P-wave velocity (Li et al.2020).

The artificial neural network is one of the most popular machine learning approaches (Hassoun et al., 1995); Zhang et al., 2021). Due to its high nonlinear mapping capability, it is often used in different prediction problems (Salehin et al., 2020). More specifically, this approach can provide an accurate estimate of different rock properties (e.g., Abdi et al., 2018; Moussas and Diamantis, 2021; Matin et al., 2018; Yesiloglu-Gultekin and Gokceoglu, 2022). In Table 1, some prediction models are summarized. Armaghani et al. (2021) used artificial neural networks (ANN) to predict granite UCS using the effective porosity and the compressional wave velocity. Yilmaz and Yuksek (2009) trained an artificial neural network model with multivariate regression analysis to predict soluble rock.

In another study, the UCS and elastic modulus of shear rock were predicted by developing a multi-layer ANN (Kahraman et al., 2009). Yagiz et al. (2012) showed that the performance of the neural network is better than that

¹ School of Electrical and Computer Engineering, College of Engineering, University of Tehran, Tehran, Iran. ² Department of Geology, Faculty of Science, Ferdowsi University of Mashhad, Mashhad, Iran, ³ Department of Geology, Faculty of Sciences, Bu-Ali Sina University, Hamedan, Iran, ⁴ Department of Geology, Faculty of Sciences, Kharazmi University, Tehran, Iran

✉ M. Amiri: a.mehrdad1372@yahoo.com

of the multivariate regression in predicting the UCS and elastic modulus of limestone from the fracture persistence index. The study by Torabi-Kaveh et al. (2015) used the rock's physical properties such as porosity, density, durability, and velocity of ultrasonic as the model input to predict the compressive strength and elastic modulus of Asmari limestone. They found that the neural network outperforms the multivariate regression analysis in the prediction task. These studies confirmed that the development of neural networks brings a new opportunity in regression tasks in engineering geology.

This study aims to estimate uniaxial compressive strength indirectly, using a deep neural network approach. Although some papers have been worked on estimating the uniaxial compressive strength using neural network models, most of the previous research focused on a specific type of rock and conducted their study with a limited number of samples. In the present study, we extend the prediction of UCS parameters for several types of rocks using a unified deep neural network framework. It is worth mentioning that, the use of various types of rocks in learning the deep network weights makes the model more generalizable and reliable. In order to consider any kind of dependency between the neurons in two sequential layers of the neural network, we use fully connected layers in the

network. Additionally, to prevent overfitting in the trained model a dropout layer is also applied.

The physical and mechanical parameters that are used as the model inputs are dry density (ρ), water absorption (I_v), ultrasonic P-wave velocity (V_p), point load test (Is_{50}), and Brazilian tensile strength (BTS). In order to reduce the redundancy of the input data and make them more statistically significant, we used a feature reduction stage before the DNN model. This makes the proposed model work easier and faster. The most popular technique for dimensionality reduction is the principal component analysis (PCA for short). This method converts the correlated features into uncorrelated variables by projecting the input data on a lower dimensional space without losing significant information. In this study, the dimensionality of the input space is reduced using PCA without any degradation in the prediction performance. The innovative aspects of this research, include the choice of DNN and its integration with PCA.

The remainder of this paper is organized as follows. The Sampling locations are introduced in Section 2. The Physical and Mechanical characteristics are presented in Section 3. The deep neural network is expressed in Section 4. The simulation results and discussions are presented in Section 5. Finally, the paper is concluded in Section 6.

Table 1 Some predictive models estimate UCS

References	Predictive Model	Input	Output
Teymen & Mengüç, 2020	Simple and multiple regression analysis, ANN, ANFIS, and genetic expression programming	$\gamma, Is_{50}, BTS, SH, R_n, V_p$	UCS
Barham et al., 2020	ANN	$V_p, SH, BTS, \rho_d, SDI,$ and PLS	UCS
Miah et al., 2020	ANN and SVM	Resistivity, gamma ray, bulk density, n , and sonic time	UCS
Armaghani et al., 2021	ANN	$n (\%), V_p$	UCS
Fang et al., 2021	ANN, hybrid ANN with imperialism competitive algorithm (ICA-ANN), hybrid ANN with artificial bee colony (ABC-ANN) and genetic programming (GP)	$n (\%), Is_{50}, R_n, V_p$	UCS
Gül et al., 2021	Multilayer Perceptron Neural Network (MLPNN), M5 Model Tree (M5MT), Extreme Learning Machine (ELM)	BTS, V_p, SH	UCS
Moussas & Diamantis, 2021	Regression analysis, ANN	$n (\%), Is_{50}, SH, V_p, Ser (\%)$	UCS
Diamantis & Moussas, 2021	Regression analysis, ANN	$\gamma_s, \gamma_d, n (\%), Is_{50}, SH, V_p$	UCS
Jain et al., 2022	ANN	-	UCS
Shahri et al., 2022	SVM-FMA	$\rho, n, V_p,$ water absorption, and PLS	UCS
Jin et al., 2022	GWO-ELM	SH, V_p, PLS, n	UCS
Moradi et al., 2022	Regression analysis	SH, ρ	UCS
Yu et al., 2023	Regression analysis, ANN, MPA	Is_{50}, RL, V_p	UCS
Asteris et al., 2024	ANN models	$n (\%), V_p, SH$	UCS

ANN: artificial neural network; SVM: support vector machine; FMA: firefly metaheuristic algorithm; ANFIS: adaptive neuro-fuzzy inference system; GEP: gene expression programming; RF: random forest DNN: deep neural networks; GP: genetic programming; ELM: extreme learning machines; GWO: grey wolf optimization.

II. SAMPLING LOCATIONS

The study areas are located in the Iranian plateau which includes four zones: Central Iran, Urumieh-Dokhtar, Sanandaj- Sirjan, and Zagros (Aghanabati, 2004). In the following, rock samples of each formation belonging to each zone are explained. The Qom Formation in the Central Iran zone is very wide and thick in the Hamedan and Saveh areas. The thickness of this formation reaches 3600 m in the west of Saveh and the north of Hamedan provinces. The above-mentioned areas have thick marl deposits and the deepest part of the Qom Formation. The marl samples are located in the northeast of Hamadan province and south of Saveh city of Markazi province. This formation in this area with Oligocene age. In the northeast of Hamadan, a wide volume of the Qom formation is developed of light gray marl. In this area, marls are the dominant part of the Qom Formation (Aghanabati, 2004). Upper Red Formation generally comprises sandstone, marl, conglomerate, and evaporate rocks. The sandstone samples are located in the east of Qom province. This formation is commonly inclined and occasionally gradually located on the Qom formation. It made up the gradual subsidence of the bed, and molasse conditions, and significantly increased thickness. The upper layers of this formation gradually changed to sandy coarse-grained and conglomerate, which probably belongs to the Pliocene (Aghanabati, 2004). The Tuff of Karaj Formation is located in Urumieh-Dokhtar zone with Eocene age in Tafresh of Markazi Province of Iran. According to the structural division of Iran, the Tafarsh area is located in the plutonic, sedimentary, and volcanic zone of Urmia Dokhtar. As following an important extensional phase made up in many parts of Iran the result was wide volcanism in the Eocene age. Volcanism in this area is generally explosive. It has formed pyroclastic units, including ignimbrite, lithic tuff, crystal tuff, and glass tuff in the area (Aghanabati, 2004). Alvand Plutonic complex is located in the Sanandaj-Sirjan zone, the most active tectonic zone in Hamadan province of western Iran. The main part of the complex is made up of granitoid rocks. Granitoid rocks, including monzogranite, granodiorite, and tonalities. This complex has an area of about 411 Km^2 and with metamorphic rocks around 711 Km^2 . The contact metamorphism in this area is due to the intrusion of the Alvand plutonic, and the regional metamorphism of the Sanandaj-Sirjan zone is caused by the activity of the Zagros orogenic belt. The Hornfelse metamorphic rocks formed adjacent to the Alvand batholith. Regional metamorphic rocks are generally developed in the eastern, northeastern, and southern parts of Alvand plutonic. These rocks include slate, phyllite, and schist (Aghanabati, 2004). The conglomerate of the Bakhtiary Formation is placed in the Zagros zone with Eocene age in the Khuzestan province

of southwest Iran. This formation is characteristic of alluvial sediments resulting from the erosion of the highlands, which generally includes conglomerate and calcareous sandstone. The cross-section of this formation in the north of Suleiman Mosque city of Khuzestan province consists of 550 m of conglomerate with fragments of gravel, cobble, and sand of various ages, which are cemented with calcite and clay (Aghanabati, 2004). The sampling site map locations of this work are shown in Fig. 1 with red stars. 221 block samples of different rock types are collected with the size of $20 \times 35 \times 35 \text{ cm}^3$ to $30 \times 40 \times 40 \text{ cm}^3$. The collected samples are phyllite, slate, schist, Hornfels, tuff, granite, sandstone, marl, and conglomerate.

III. RESEARCH METHODOLOGY

In this study, rock samples were collected from different areas of Iran. These samples have none or are slightly weathered. The physical and mechanical properties of igneous (granite), sedimentary (sandstone, marl, and conglomerate), and metamorphic (phyllite, slate, schist, Hornfels, tuff) rocks were determined based on the International Society for Rock Mechanics (ISRM) and American Society for Testing and Materials (ASTM) methods, after a systematic grouping, the data related to each rock type. The validation of the presented relationships was verified using modern methods. Then, a multi-layer neural network was designed using Python software. Finally, the uniaxial compressive strength was estimated by using the designed artificial neural network. In the following, the details of these tests and analyses were presented.

A. Physical characteristics

The evaluation of the physical characteristics of rock is serious in engineering geology, mining, and civil projects. These characteristics rely on the micro-cracks and mineral content of the intact rock- micro cracks, including cleavage plane and grain boundaries, which rock strength decreased with an increase in them. In addition, Mineral contents, including feldspar, calcite, quartz, muscovite, biotite, and clay minerals, have been influenced by the type, percentage, composition of minerals, and texture (Willard and McWilliams 1969; Shalabi et al. 2007; Karrari et al. 2023; Asteris et al., 2024). In the current research, the physical properties of the rock samples, including the dry density (ρ), and water absorption (I_p ,%) were determined by using of International Society for Rock Mechanics method (ISRM 2007). 221 tests of physical properties were performed on cylindrical specimens. The dry density of tested rocks ranges from $2.35 \pm 0.27 \text{ gr/cm}^3$ to $2.80 \pm 0.009 \text{ gr/}$

cm^3 , respectively. According to the Anon (1977) classification, the dry density values were medium to very high. The water absorption of tested rocks ranges from 0.40% to 6.19%, respectively. Based on the ASTM (1999) classification, the water absorption values were low to medium. The sandstone and hornfel samples had the lowest and highest values for dry unit weight, while the Phyllite and Marl samples had the lowest and highest values for water absorption, respectively. The physical properties and their statistical information along with the number of samples for each rock type are shown in Table 2.

B. Mechanical characteristics

The mechanical characteristics of rock are related to physical properties (Bandini and Berry 2013). The relationship between both rock properties makes it probable to forecast the strength of the intact rock, that it can be applied in the initial design of the tunneling, mining, and civil project with less cost and time, and simple tests. The mechanical parameters include ultrasonic P -wave velocity (V_p), point load test (Is_{50}), Brazilian tensile strength (BTS), and uniaxial compressive strength (UCS). The physical and mechanical characteristics of rocks are used to predict the UCS. The mechanical characteristics of the samples are presented in Table 3. As follows, the mechanical characteristics are explained.

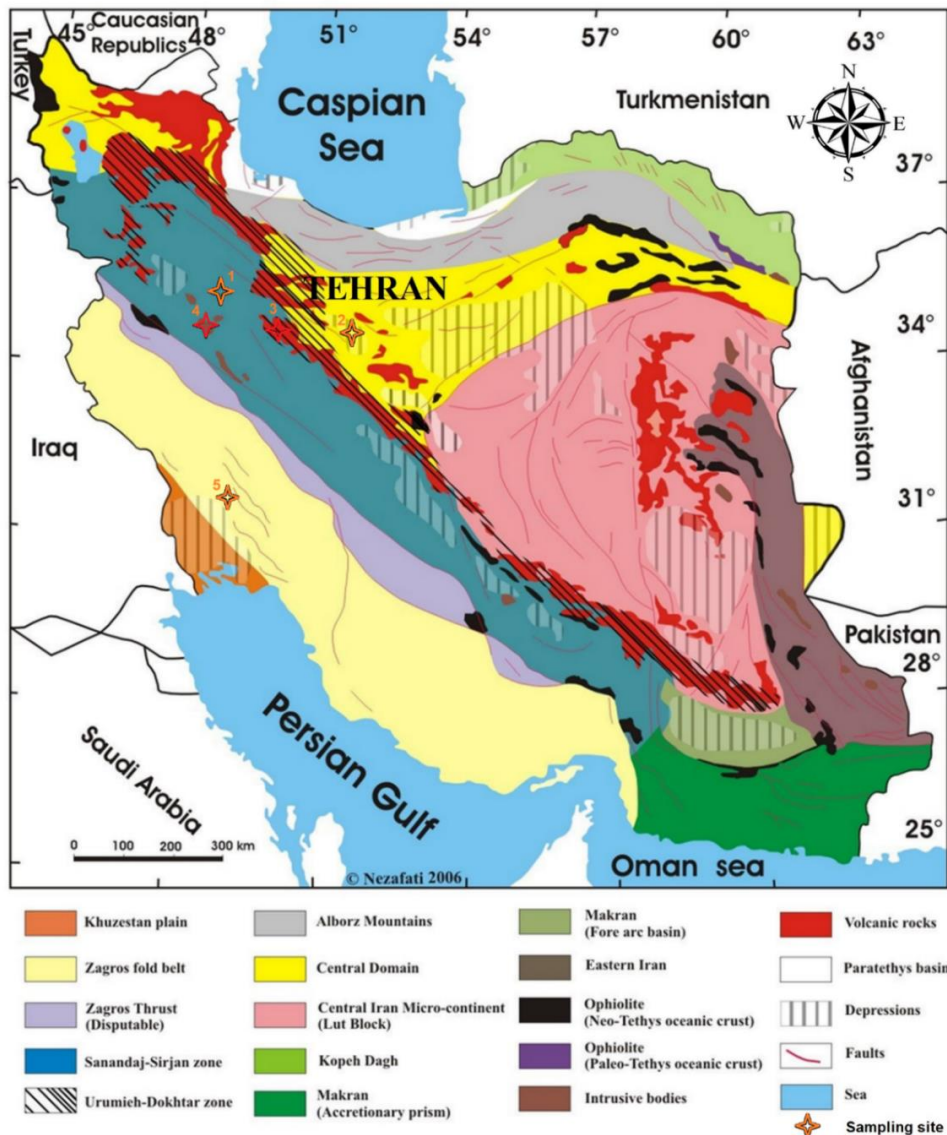


Fig. 1. Sampling site map (Stocklin and Nabavi, 1973 Modified). The red stars indicate the sampling site group: 1. Marl samples of Qom Formation; 2. sandstone of Upper Red Formation; 3. Tuff of Karaj Formation; 4. Alvand Plutonic complex; 5. conglomerate of Bakhtiari Formation.

1) *P-wave Velocity*

The ultrasonic wave velocity was quantified in the laboratory based on ASTM D2845 (1983). This method is frequently used to determine the dynamic properties of rocks. As this method is simple and nondestructive to apply, it is being more used in geological engineering. The P-wave velocity depends on different factors such as mineral content, porosity, density, micro-cracks, and weathering (Goodman, 1989; Karrari et al., 2023; Asteris et al., 2024). The P-wave velocity values range from 2272.76 to 4576.87 m/s. According to the IAEG (1979) classification, the P-wave velocity values were very low to high. The Schist and Hornfels samples had the lowest and highest wave velocities, respectively.

2) *Point Load Index*

The point load test is usually applied to the comfort of testing, and the possibility of field usability. This test is often used as an indirect method to measure the compressive strength of rocks (Kahraman and Gunaydin 2009). Axial point load tests were carried out to determine the point load index (Is_{50}). The test was performed on the core samples with 54.7 mm diameter and a length/diameter ratio of $\sim 1:2$. The point load index for a core diameter equal to 50 mm (Is_{50}) is calculated as follows:

$$Is_{50} = F \frac{P}{D_e^2} \quad (1)$$

$$F = \left(\frac{D_e}{50}\right)^{0.45} \quad (2)$$

$$D_e^2 = \frac{4A}{\pi} \quad (3)$$

$$A = W \times D \quad (4)$$

Where P , D_e , F , W , and D denote the peak load, equivalent core diameter, and size correction factor, the smallest specimen width perpendicular to the loading direction, and the distance between the platens at failure, respectively (Jamshidi et al. 2020). The point load test was conducted according to the standard ISRM (2007). The point load test values range from 1.39 to 6.85 MPa. According to the Deer (1968) classification, the point load values range from very low to high. According to the Bieniawski (1973) classification, the point load values range from low to high. The Slate and Hornfels samples had the lowest and highest point load index, respectively.

3) *Brazilian Tensile Strength*

The Brazilian tensile strength is an indirect testing method for gaining the tensile strength of rock (Li and Wong 2013). ISRM (1978), ASTM-D-3967 (2001b), and ISRM (2007) recommended methods for determining Brazilian tensile strength. According to the ISRM (2007), this test was conducted on specimens with

length/diameter ratios between 0.5 and 0.75. The BTS parameter is computed using the following equation:

$$BTS = 2P/\pi Dt \quad (5)$$

Where P , D , and t are the peak load, diameter, and thickness of the disc, respectively (Jamshidi et al., 2020). In this research, according to ISRM (2007), the point load test values range from 2.75 to 11.21 MPa. According to the results, the Phyllite and Tuff samples had the lowest and highest BTS values, respectively.

4) *Uniaxial compressive strength*

The UCS test is generally used in rock mechanics. ASTM-D-2938 (1995), ISRM (1979), and ISRM (2007) define the suggested method for quantification of UCS. Application of point load, Brazilian Tensile Strength, P-wave Velocity, and physical characteristics may be used for indirect method determination of UCS (Cargill and Shakoor 1990; Karrari et al. 2023; Asteris et al., 2024). The results of the physical, mechanical, and dynamical properties of samples are presented in Tables 1 and 2, respectively. Hornfels and sandstone samples had the highest and lowest density (ρ), respectively. Marl samples had the highest water absorption (I_v). Hornfels and phyllite had the lowest water absorption. The P-wave Velocity of Hornfels had the highest value. Brazilian Tensile Strength of Phyllite and Tuff had the lowest and highest value. Hornfels and Slate had the highest and lowest Point Load Strength, respectively.

The uniaxial compressive strength tests were conducted on 54.7 mm core samples with a length-to-diameter ratio 2.5. The loading was applied with a rate of 0.5-1 MPa/s. The UCS test was conducted according to the standard ISRM (2007). The UCS test values range from 22.37 to 107.92 MPa. According to the ISRM (2007) classification, The UCS values range from medium to high. The Slate and Tuff samples had the lowest and highest UCS, respectively. All the input parameters of the model and the target UCS values are plotted in Fig. 2. Test results are shown in Table 3.

IV. DEEP NEURAL NETWORK

The simplest neural network model is the single-layer network that involves I linear combinations of the input features. This neural network can be formulated as follows:

$$z_i = \sum_{j=1}^D w_{ij} f_j + b_i, \quad i = 1, \dots, I \quad (6)$$

Where f_j is the j th input feature, b_i , and z_i are the i th bias and the i th output of the NN model, respectively. w_{ij} is the weight from the j th input to the i th output. The outputs of each layer are passed through an appropriate activation function.

$$a_i = h(z_i), \quad i = 1, \dots, I \quad (7)$$

Where a_i is the output of the i th neuron on a layer and I is the total number of neurons. The bias parameters can be viewed as a set of weights and their corresponding input features are equal to one. Therefore, the equations 6 and 7 are written as follows.

$$a_i = h(\sum_{j=0}^D w_{ij} f_j) \quad (8)$$

where $f_0 = 1$ and $w_{i0} = b_i$. We can rewrite 8 in a matrix form as:

$$a = h(z) \quad (9)$$

And

$$z = Wf \quad (10)$$

where $a = [a_1, \dots, a_I]^T$, $z = [z_1, \dots, z_I]^T$, $f = [1, f_1, \dots, f_D]^T$, and the weight matrix is defined as follows:

$$W = \begin{bmatrix} w_{10} & \dots & w_{1D} \\ \vdots & \ddots & \vdots \\ w_{I0} & \dots & w_{ID} \end{bmatrix} \quad (11)$$

Note that 9 and 10 can be extended to NN with any number of hidden layers. The output of the n th layer can be expressed as:

$$a^{(n)} = h^{(n)}(z^{(n)}) \quad (12)$$

Where

$$z^{(n)} = W^{(n)} a^{(n-1)} \quad (13)$$

In which the initial parameter $a^{(0)}$ is equal to f .

Table 2 Physical properties and number of samples.

Rock type	Statistical properties	Phyllite	Slate	Schist	Hornfels	Tuff	Granite	Sandstone	Marl	Conglomerate
Sample N		7	7	7	14	44	7	58	69	8
ρ (gr/cm ³)	Max	2.73	2.72	2.56	2.81	2.64	2.76	2.75	2.58	2.60
	Min	2.72	2.70	2.54	2.79	2.24	2.58	1.73	2	2.53
	Avg	2.73 ± 0.005	2.71 ± 0.005	2.55 ± 0.005	2.80 ± 0.009	2.48 ± 0.08	2.66 ± 0.061	2.35 ± 0.27	2.36 ± 0.14	2.56 ± 0.02
I_v (%)	Max	0.4	1.30	3.50	4.1	4.6	0.92	10	8.35	1.49
	Min	0.4	1.36	3.60	4	0.13	0.15	0.53	4	0.93
	Avg	0.40	1.33	3.55	0.405 ± 0.005	2.18 ± 1.41	0.51 ± 0.22	3.86 ± 3.95	6.19 ± 2.05	1.18 ± 0.21

Table 3 Values of dynamical and mechanical properties of samples.

Rock type	Statistical properties	Phyllite	Slate	Schist	Hornfels	Tuff	Granite	Sandstone	Marl	Conglomerate
Sample N		7	7	7	14	44	7	58	69	8
BTS (MPa)	Max	5.46	7.43	5.09	21.9	28.44	11.22	13.23	8.88	6.57
	Min	1.03	1.33	3.38	5.58	4.4	3.82	0.84	1.93	5.03
	Avg	2.75 ± 1.83	2.84 ± 2.08	3.97 ± 0.69	10.93 ± 5.23	11.21 ± 5.97	7.57 ± 2.81	6.03 ± 3.49	3.37 ± 1.24	5.60 ± 0.5
V_p (m/s)	Max	5741.48	6248.41	3142.86	5487.33	5344	5500	4880	3350	4730
	Min	2195.2	1713.51	1516.21	3316.73	2833	2570	867	1880	4044
	Avg	3629.76 ± 1444.84	3518.337 ± 1634.82	2272.76 ± 403.33	4576.87 ± 673.76	3900.97 ± 706.09	4168.57 ± 1168.9	3016.47 ± 1315.2	2942.12 ± 398.92	4347.37 ± 282.62
Is_{50} (MPa)	Max	3.66	2.51	1.83	9.8	10.38	7.32	7.63	6.22	5.75
	Min	0.64	0.76	1.01	2.8	1.9	2.52	0.47	1.09	3.96
	Avg	1.7 ± 1.08	1.39 ± 0.67	1.43 ± 0.32	6.85 ± 2.24	4.74 ± 2.19	4.7 ± 1.64	4.07 ± 2.39	3.06 ± 1.01	4.82 ± 0.58
UCS (MPa)	Max	47.38	43.87	35.52	172.59	205.4	123	143.03	83.11	68.13
	Min	5.65	6.02	17.83	44.02	39	61.58	5.81	19.34	37.48
	Avg	26.37 ± 16.75	22.37 ± 14.23	24.46 ± 6.18	100.78 ± 38.23	107.92 ± 42.62	99.56 ± 23.78	70.81 ± 38.56	50.80 ± 11.71	50.24 ± 9.41

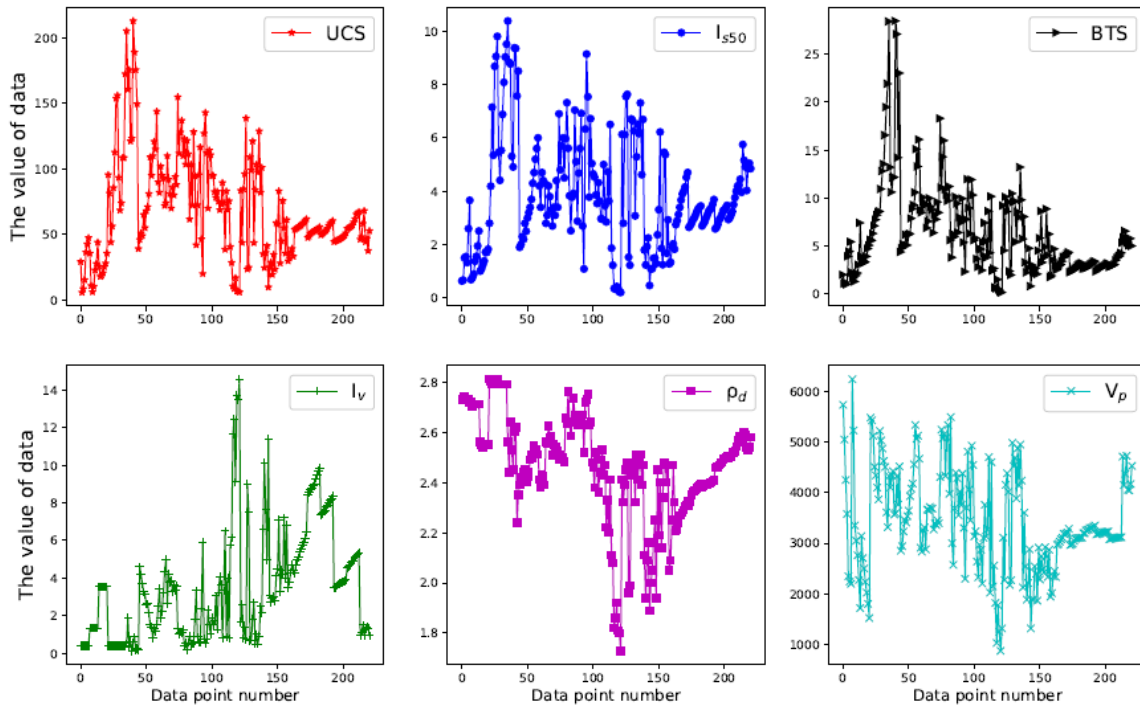


Fig. 2. The value of physical and mechanical properties of data samples in this study.

A. Activation function

An activation function (AF) in a NN is defined as how the weighted sum of the inputs is transformed into the output of a node or nodes in a hidden layer. There are many different types of activation functions, including the Rectified Linear Activation (ReLU), the Logistic (Sigmoid), the Hyperbolic Tangent (Tanh), and the linear function. The type of activation function is chosen based on the neural network architecture. In this study, the Tanh function and linear function are applied for the hidden layers and the output layer, respectively. The Hyperbolic tangent (tanh) function is

$$h(x) = \tanh(x) = \frac{e^x - e^{-x}}{e^x + e^{-x}} \quad (14)$$

Where the range of the output is $(-1, 1)$ and the linear function is

$$h(x) = x \quad (15)$$

Where the range of the output is $(-\infty, \infty)$.

B. Pre-processing data

The primary goal of pre-processing is to manipulate and prepare data for the following processing stages. Pre-processing of the dataset is an important step since it enhances the quality of the data. In this study, each feature extracted from the dataset is scaled and translated individually such that it falls in the range between zero and one. Consequently, the features are normalized as follows.

$$x_n = \frac{x - x_{min}}{x_{max} - x_{min}} \quad (16)$$

Where x_{min} and x_{max} are the minimum and the maximum values for each training feature, respectively, and x_n is the normalized feature.

C. Proposed deep neural network model

The proposed DNN structure is shown in Fig. 3. This network has an input layer, four hidden layers, and an output layer. In order to prevent overfitting in the trained model, a dropout layer is used in the network. This layer sets the outputs of some randomly selected neurons to zero. As shown in Fig. 3, before the input layer of the DNN, a feature reduction stage is applied to reduce the number of input features to the neural network model. Note that fewer input features can result in a more straightforward prediction model with the same performance and lower computational complexity. One of the popular unsupervised techniques for dimensionality reduction is the principle component analysis (PCA). This method converts the correlated features into uncorrelated variables by projecting the input data on a lower dimensional space while preserving the maximum amount of information (Yang et al., 2004; Abdi and Williams, 2010; Mackiewicz and Ratajczak, 1993). PCA can be implemented by computing the eigenvectors corresponding to the largest eigenvalues of the covariance matrix of the feature vectors. In PCA, the principal components correspond to the directions with the largest variances of the dataset. In order to choose the appropriate number of principal components, the cumulative explained variance ratio criterion is applied, which is defined as follows.

$$V_n = \frac{\sum_{j=1}^n \lambda_j}{\sum_{i=1}^{C_t} \lambda_i} \quad (17)$$

Where V_n is the percentage of the cumulative variance of the n selected components. λ_j and C_t are the j th sorted eigenvalue of the data and the total number of components, respectively.

V. SIMULATION RESULTS

In this part, the performance of the proposed DNN with PCA feature reduction is evaluated using the Leave-One-Out (LOO) cross-validation. The LOO method uses all but one data as the training data and leaves one sample for the test. This evaluation process was repeated for each of the 221 samples, ensuring that every sample was utilized as test data exactly once. The evaluation is repeated for each data sample as the test data. All simulations are performed in Python 3 software on an Intel(R) Core (TM) i5-6200U CPU at 2.30 GHz and 8GB RAM. The best model was determined based on its performance metrics, including accuracy, root mean square error (RMSE), and correlation coefficient (CC), all evaluated during the LOO validation process. These metrics offered a comprehensive assessment of the model's predictive capability. The model with the lowest RMSE and the highest CC values across all iterations was selected as the best.

Fig. 4 shows the loss curves for the train and validation data in the DNN model. It can be seen that from epoch 20, the network losses converge to their final values. In this figure and the following results, the model performance is evaluated using the mean square error (MSE) criterion.

In order to understand the required number of components in the PCA algorithm, the cumulative variance ratio curve is shown in Fig. 5. According to the results in Fig. 5, more than 80% of the feature variance

is kept in only two components. Accordingly, we only use two principal components, and consequently, the input dimension of the DNN model is selected to be two.

Fig. 6 shows the MSE of the UCS prediction using the proposed DNN for a different number of components. The results show that reducing the number of components from five to two does not lead to significant degradation in prediction performance.

The MSE of the DNN method with and without the feature reduction stage were 0.0068 ± 0.001 and 0.0067 ± 0.013 , respectively. Similar to the results in the Fig. 6, this shows that the dimension of the input vector can be reduced from five to two without any significant degradation in the network performance. It is worth noting that, in previous studies for the prediction of the UCS from different rock properties, the highly correlated features are manually mitted by computing the correlation matrix (Manouchehrian et al., 2012; Moussas and Diamantis, 2021; Tang and Na, 2021), but this is not required in this study since the PCA algorithm automatically decorrelate the features in the reduced dimensional space.

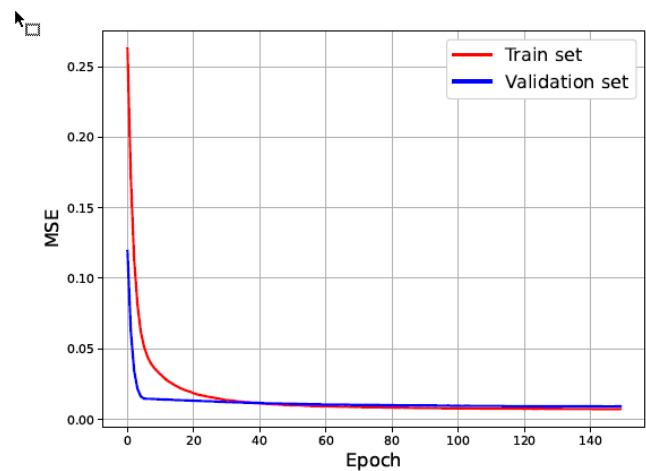


Fig. 4. The loss curves of the network for the training and validation data

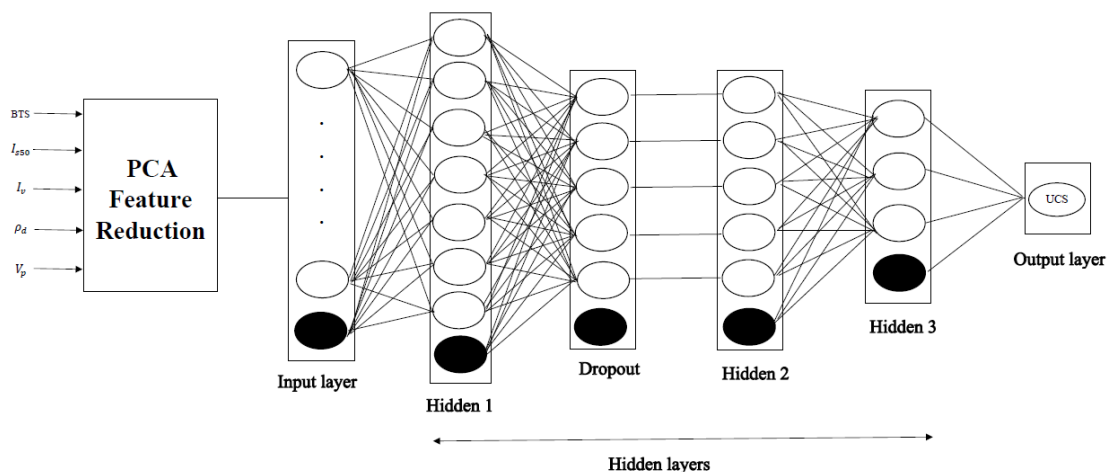


Fig. 3. The structure of the proposed DNN for prediction of the uniaxial compressive strength

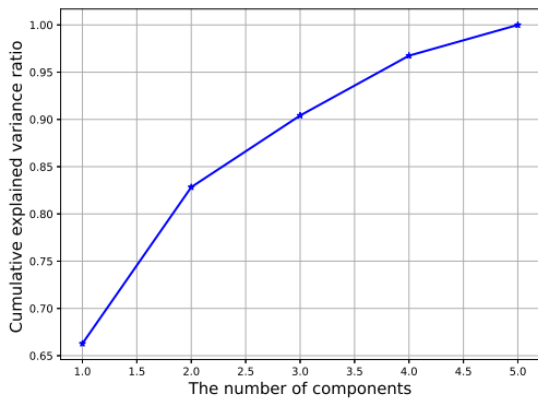


Fig. 5. The cumulative variance ratio for different numbers of components.

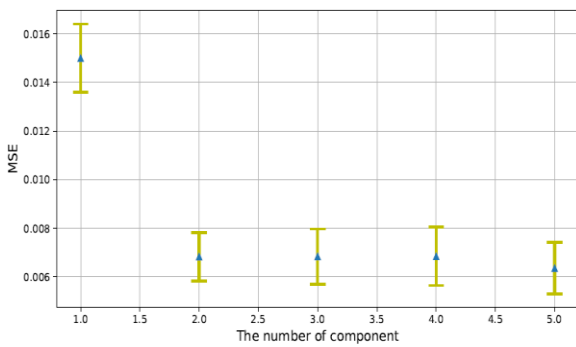


Fig. 6. The MSE UCS prediction versus the applied number of components in the feature reduction step using the PCA algorithm

Fig. 7. illustrates the scatter plot of the predicted UCS versus the measured values for all types of rocks. The vertical distance between each point in Fig. 7 and the reference black line is the regression error. The scatter plot depicts that the hornfels rocks (the blue stars) have the largest prediction error. In order to quantify the prediction error of different types of rocks, Fig. 8, the MSE and the standard deviation of UCS prediction error are evaluated for each type of rock. It can be seen that marl and hornfels have the minimum and maximum values of MSE, respectively.

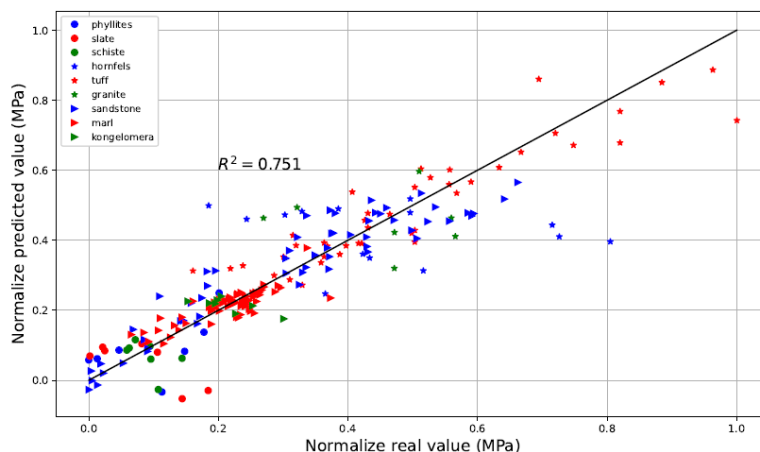


Fig. 7. Scatter plot of the predicted versus measured UCS values using DNN

The UCS of intact rocks is essential for various engineering applications (such as constructions, geotechnical projects, and historic buildings that lack sufficient core samples). The main important rock engineering parameters are cumbersome, difficult, and costly, requiring a large budget and a long time to estimate in different rocks. Therefore, the prediction of this parameter using simpler, cheaper indirect methods is of interest. In this research, different types of rocks were predicted using one unified deep neural network framework. However, the previous research focused on a specific type of rock and conducted their study with a limited number of samples. For future research, suggest applying different methods such as least squares support vector machine (RF, SVM, GEP, etc) and many rock types.

VI. CONCLUSION

In this study, was estimated the uniaxial compressive strength of rocks by using machine learning. 221 block samples of different rock types were collected from five Formation and complexes of Iran as follows: Marl samples of Qom Formation; Sandstone of Upper Red Formation; Tuff of Karaj Formation; conglomerate of Bakhtiary Formation, and Alvand Plutonic complex. This study presented a deep neural network to predict the uniaxial compressive strength in different rocks of Iran. The proposed network was designed to indirectly predict the UCS using the physical and mechanical properties of rocks. This avoided the time-consuming and expensive tests for measuring the UCS. The principle component analysis was used to reduce the dimension of the input data and increase the generalization power of the model. Simulation results show that PCA can reduce the input features without any degradation in the performance of the DNN model. The results indicated that the combination of the PCA and the suggested DNN model is effective and useful in predicting UCS. The MSE of the proposed method with and without the feature reduction step were 0.0068 ± 0.001 and 0.0067 ± 0.013 , respectively.

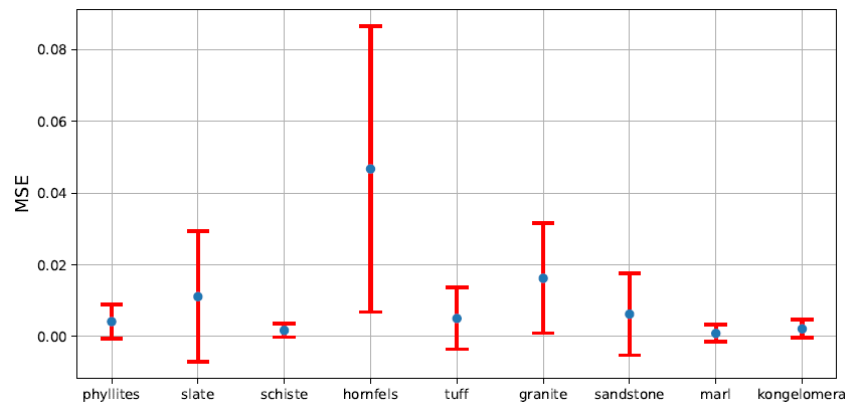


Fig. 8. The MSE for prediction of each type of rock

References

- Abbaszadeh Shahri, A., Maghsoudi Moud, F., & Mirfallah Lialestani, S. P. (2022). A hybrid computing model to predict rock strength index properties using support vector regression. *Engineering with Computers*, 38(1), 579-594.
- Abdi, H. Williams., LJ (2010). *Principal Component Analysis*. Wiley Interdisciplinary Reviews: Computational Statistics.
- Abdi, Y., Garavand, A. T., & Sahamieh, R. Z. (2018). Prediction of strength parameters of sedimentary rocks using artificial neural networks and regression analysis. *Arabian Journal of Geosciences*, 11, 1-11.
- Aghanabati, S. A. (2004). *Geology of Iran*. Geological Survey and Mining Exploration of Iran, Tehran. 586p.
- Anon (1979) Classification of rocks and soils for engineering geological mapping, part: Rack and soil materials. Report of the Commission of Engineering Geological Mapping, Bulletin International Association of Engineering Geology, 19: 364-371.
- Armaghani, D. J., Mamou, A., Maraveas, C., Roussis, P. C., Siorikis, V. G., Skentou, A. D., & Asteris, P. G. (2021). Predicting the unconfined compressive strength of granite using only two non-destructive test indexes. *Geomech. Eng*, 25(4), 317-330.
- ASTM (1983) Test methods for ultraviolet velocities determination. *Am Soc Test Mater* D2845.
- Asteris, P. G., Karoglou, M., Skentou, A. D., Vasconcelos, G., He, M., Bakolas, A., & Armaghani, D. J. (2024). Predicting uniaxial compressive strength of rocks using ANN models: Incorporating porosity, compressional wave velocity, and Schmidt hammer data. *Ultrasonics*, 141, 107347. <https://doi.org/10.1016/j.ultras.2024.107347>
- Bandini, A., & Berry, P. (2013). Influence of marble's texture on its mechanical behavior. *Rock mechanics and rock engineering*, 46, 785-799.
- Bieniawski, Z. T. (1973). Engineering classification of jointed rock masses. *Civil Engineering= Siviele Ingenieurswese*, 1973(12), 335-343.
- Bieniawski, Z. T., & Bernede, M. J. (1979, April). Suggested methods for determining the uniaxial compressive strength and deformability of rock materials: Part 1. Suggested method for determining deformability of rock materials in uniaxial compression. In *International Journal of Rock Mechanics and Mining Sciences & Geomechanics Abstracts* (Vol. 16, No. 2, pp. 138-140). Pergamon.
- Barham, W. S., Rabab'ah, S. R., Aldeeky, H. H., & Al Hattamleh, O. H. (2020). Mechanical and physical-based artificial neural network models for the prediction of the unconfined compressive strength of rock. *Geotechnical and Geological Engineering*, 38, 4779-4792.
- Bieniawski, Z. T., & Hawkes, I. (1978). International-Society-for-Rock-Mechanics-Commission-on-Standardization-of-Laboratory-and-Field-tests-suggested methods for determining tensile-strength of rock materials. *International Journal of Rock Mechanics and Mining Sciences*, 15(3), 99-103.
- Cargill, J. S., & Shakoor, A. (1990, December). Evaluation of empirical methods for measuring the uniaxial compressive strength of rock. In *International Journal of Rock Mechanics and Mining Sciences & Geomechanics Abstracts* (Vol. 27, No. 6, pp. 495-503). Pergamon.
- Deere, D. U., & Deere, D. W. (1989). Rock quality designation (RQD) after twenty years (No. 89). *US Army Engineer Waterways Experiment Station*.
- Diamantis, K., & Moussas, V. C. (2021). Estimating uniaxial compressive strength of peridotites from simple tests using neural networks. *Arabian Journal of Geosciences*, 14, 1-13.
- Diamantis, K., Gartzos, E., & Migiros, G. (2009). Study on uniaxial compressive strength, point load strength index, dynamic and physical properties of serpentinites from Central Greece: test results and empirical relations. *Engineering Geology*, 108(3-4), 199-207.
- Fang, Q., Yazdani Bejarbaneh, B., Vatandoust, M., Jahed Armaghani, D., Ramesh Murlidhar, B., & Tonnizam Mohamad, E. (2021). Strength evaluation of granite block samples with different predictive models. *Engineering with computers*, 37, 891-908.
- Fener, M. U. S. T. A. F. A., Kahraman, S. A. İ. R., Bilgil, A., & Gunaydin, O. (2005). A comparative evaluation of indirect methods to estimate the compressive strength of rocks. *Rock Mechanics and Rock Engineering*, 38, 329-343.
- Goodman, R. E. (1991). *Introduction to rock mechanics*. John Wiley & Sons.
- Gül, E., Ozdemir, E., & Sarıcı, D. E. (2021). Modeling uniaxial compressive strength of some rocks from Turkey using soft computing techniques. *Measurement*, 171, 108781.
- Hassoun, M. H. (1995). *Fundamentals of artificial neural networks*. MIT Press.
- Heidari, M., Khanlari, G. R., Torabi Kaveh, M., & Kargarian, S. (2012). Predicting the uniaxial compressive and tensile strengths of gypsum rock by point load testing. *Rock mechanics and rock engineering*, 45, 265-273.
- ISRM (1978) Suggested methods for determining tensile strength of rock materials. Suggested method for determining indirect tensile strength by Brazilian test. Commission on Standardization of Laboratory and Field Tests. Z.T. Bieniawski and I. Haweks. *Int J Rock Mech Min Sci Geomech Abstr* 15:102-103
- ISRM (1979) Suggested methods for determining the uniaxial compressive strength and deformability of rock materials. *Int J Rock Mech Min Sci* 16(2):135-140.
- ISRM (2007) *The blue book: the complete ISRM suggested methods for rock characterization, testing and monitoring: 1974-2006*. In: Ulusay R, Hudson JA (eds) *Compilation arranged by the ISRM Turkish National Group*, Ankara, Turkey. Kazan Offset Press, Ankara.
- Jamshidi, A., Abdi, Y., & Sarikhani, R. (2020). Prediction of brittleness indices of sandstones using a novel physico-mechanical parameter. *Geotechnical and Geological Engineering*, 38, 4651-4659.
- Jin, X., Zhao, R., & Ma, Y. (2022). Application of a Hybrid Machine Learning Model for the Prediction of Compressive Strength and Elastic Modulus of Rocks. *Minerals*, 12(12), 1506.
- Jain, D., Bhadauria, S. S., & Kushwah, S. S. (2022). Prediction of Compressive Strength of Plastic Composite Construction Material Using Artificial Neural Network. In *International Conference on Recent Advances in Civil Engineering* (pp. 235-239). Singapore: Springer Nature Singapore.

- Kahraman, S., & Gunaydin, O. (2009). The effect of rock classes on the relation between uniaxial compressive strength and point load index. *Bulletin of engineering geology and the environment*, 68, 345-353.
- Kahraman, S., Gunaydin, O., Alber, M., & Fener, M. (2009). Evaluating the strength and deformability properties of Misis fault breccia using artificial neural networks. *Expert Systems with Applications*, 36(3), 6874-6878.
- Karrari, S. S., Heidari, M., Khademi Hamidi, J., Sharifi Teshnizi, E., 2023. Predicting geomechanical, abrasivity, and drillability properties in some igneous rocks using fabric features and petrographic indexes. *Bulletin of Engineering Geology and the Environment*, 82, 124. <https://doi.org/10.1007/s10064-023-03144-0>
- Kumar, B. R., Vardhan, H., Govindaraj, M., & Vijay, G. S. (2013). Regression analysis and ANN models to predict rock properties from sound levels produced during drilling. *International Journal of Rock Mechanics and Mining Sciences*, 58, 61-72.
- Li, D., & Wong, L. N. Y. (2013). The Brazilian disc test for rock mechanics applications: review and new insights. *Rock mechanics and rock engineering*, 46, 269-287.
- Li, D., Armaghani, D. J., Zhou, J., Lai, S. H., & Hasanipanah, M. (2020). A GMDH predictive model to predict rock material strength using three non-destructive tests. *Journal of Nondestructive Evaluation*, 39, 1-14.
- Maćkiewicz, A., & Ratajczak, W. (1993). Principal components analysis (PCA). *Computers & Geosciences*, 19(3), 303-342.
- Miah, M. I., Ahmed, S., Zendehboudi, S., & Butt, S. (2020). Machine learning approach to model rock strength: prediction and variable selection with aid of log data. *Rock Mechanics and Rock Engineering*, 53, 4691-4715.
- Manouchehrian, A., Sharifzadeh, M., & Moghadam, R. H. (2012). Application of artificial neural networks and multivariate statistics to estimate UCS using textural characteristics. *International Journal of Mining Science and Technology*, 22(2), 229-236.
- Matin, S. S., Farahzadi, L., Makaremi, S., Chelgani, S. C., & Sattari, G. H. (2018). Variable selection and prediction of uniaxial compressive strength and modulus of elasticity by random forest. *Applied Soft Computing*, 70, 980-987.
- Moussas, V. C., & Diamantis, K. (2021). Predicting uniaxial compressive strength of serpentinites through physical, dynamic and mechanical properties using neural networks. *Journal of Rock Mechanics and Geotechnical Engineering*, 13(1), 167-175.
- Moradi, S., Amiri, M., Rahimi Shahid, M. and Karrari, S. S. (2022). The presentation of simple and multiple regression relationships to the evaluation of uniaxial compressive strength sedimentary and pyroclastic rocks with usage experimental of the Schmidt hammer. *New Findings in Applied Geology*, 16(32), 92-108.
- Nefeslioglu, H. A. (2013). Evaluation of geo-mechanical properties of very weak and weak rock materials by using non-destructive techniques: ultrasonic pulse velocity measurements and reflectance spectroscopy. *Engineering Geology*, 160, 8-20.
- Ozcelik, Y., Bayram, F., & Yasitli, N. E. (2013). Prediction of engineering properties of rocks from microscopic data. *Arabian Journal of Geosciences*, 6, 3651-3668.
- Salehin, S., Hadavandi, E., & Chelgani, S. C. (2020). Exploring relationships between mechanical properties of marl core samples by a coupling of mutual information and predictive ensemble model. *Modeling Earth Systems and Environment*, 6, 575-583.
- Shalabi, F. I., Cording, E. J., & Al-Hattamleh, O. H. (2007). Estimation of rock engineering properties using hardness tests. *Engineering Geology*, 90(3-4), 138-147.
- Singh, T. N., & Dubey, R. K. (2000). Study of transmission velocity of primary wave (P-wave) in coal measure sandstone.
- Stocklin, J., & Nabavi, M. H. (1973). Tectonic map of Iran. *Geological Survey of Iran*, 1(5).
- Tang, L., & Na, S. (2021). Comparison of machine learning methods for ground settlement prediction with different tunneling datasets. *Journal of Rock Mechanics and Geotechnical Engineering*, 13(6), 1274-1289.
- Teymen, A., & Mengüç, E. C. (2020). Comparative evaluation of different statistical tools for the prediction of uniaxial compressive strength of rocks. *International Journal of Mining Science and Technology*, 30(6), 785-797.
- Tiryaki, B. (2008). Predicting intact rock strength for mechanical excavation using multivariate statistics, artificial neural networks, and regression trees. *Engineering Geology*, 99(1-2), 51-60.
- Torabi-Kaveh, M., Naseri, F., Saneie, S., & Sarshari, B. (2015). Application of artificial neural networks and multivariate statistics to predict UCS and E using physical properties of Asmari limestones. *Arabian Journal of Geosciences*, 8, 2889-2897.
- Ulusay, R., & Hudson, J. A. (2007). ISRM: The complete ISRM suggested methods for rock characterization, testing and monitoring: 1974-2006. *Kozan Ofset Matbaacılık San ve Tic Sti, Ankara*.
- Willard, R. J., & McWilliams, J. R. (1969, January). Microstructural techniques in the study of physical properties of rock. In *International Journal of Rock Mechanics and Mining Sciences & Geomechanics Abstracts (Vol. 6, No. 1, pp. 1-12)*. Pergamon.
- Yagiz, S., Sezer, E. A., & Gokceoglu, C. (2012). Artificial neural networks and nonlinear regression techniques to assess the influence of slake durability cycles on the prediction of uniaxial compressive strength and modulus of elasticity for carbonate rocks. *International Journal for Numerical and Analytical Methods in Geomechanics*, 36(14), 1636-1650.
- Yang, J., Zhang, D., Frangi, A. F., & Yang, J. Y. (2004). Two-dimensional PCA: a new approach to appearance-based face representation and recognition. *IEEE transactions on pattern analysis and machine intelligence*, 26(1), 131-137.
- Yesiloglu-Gultekin, N., & Gokceoglu, C. (2022). A comparison among some non-linear prediction tools on indirect determination of uniaxial compressive strength and modulus of elasticity of basalt. *Journal of Nondestructive Evaluation*, 41(1), 10.
- Yilmaz, I., & Yuksek, G. (2009). Prediction of the strength and elasticity modulus of gypsum using multiple regression, ANN, and ANFIS models. *International journal of rock mechanics and mining sciences*, 46(4), 803-810.
- Yu, Z., Zhou, J., & Hu, L. (2023). Prediction of compressive strength of granite: use of machine learning techniques and intelligent system. *Earth Science Informatics*, 1-17.
- Zhang, W., Li, H., Li, Y., Liu, H., Chen, Y., & Ding, X. (2021). Application of deep learning algorithms in geotechnical engineering: a short critical review. *Artificial Intelligence Review*, 1-41.